Taylor & Francis
Taylor & Francis Group

Corrosion Engineering, Science and Technology
The International Journal of Corrosion Processes and Corrosion Control

ISSN: 1478-422X (Print) 1743-2782 (Online) Journal homepage: https://www.tandfonline.com/loi/ycst20

Microbially influenced corrosion of carbon steel in the presence of anaerobic sulphate-reducing bacteria

Tomáš Černoušek, Rojina Shrestha, Hana Kovářová, Roman Špánek, Alena Ševců, Kristína Sihelská, Jakub Kokinda, Jan Stoulil & Jana Steinová

To cite this article: Tomáš Černoušek, Rojina Shrestha, Hana Kovářová, Roman Špánek, Alena Ševců, Kristína Sihelská, Jakub Kokinda, Jan Stoulil & Jana Steinová (2019): Microbially influenced corrosion of carbon steel in the presence of anaerobic sulphate-reducing bacteria, Corrosion Engineering, Science and Technology, DOI: 10.1080/1478422X.2019.1700642

To link to this article: https://doi.org/10.1080/1478422X.2019.1700642

Published online: 06 Dec 2019.

Submit your article to this journal

Article views: 8

View related articles

View Crossmark data

Full Terms & Conditions of access and use can be found at
https://www.tandfonline.com/action/journalInformation?journalCode=ycst20

CORROSION ENGINEERING, SCIENCE AND TECHNOLOGY
https://doi.org/10.1080/1478422X.2019.1700642

The Institute of Materials, Minerals and Mining

Taylor & Francis
Taylor & Francis Group

Check for updates

Microbially influenced corrosion of carbon steel in the presence of anaerobic sulphate-reducing bacteria

Tomáš Černoušek [a], Rojina Shrestha [b], Hana Kovářová [a], Roman Špánek [b], Alena Ševců [b], Kristína Sihelská [a], Jakub Kokinda [a], Jan Stoulil [c] and Jana Steinová [b,d]

[a]Department of Nuclear Fuel Cycle, Research Center Řež, Husinec, Czech Republic; [b]Institute for Nanomaterials, Advanced Technologies and Innovations, Technical University of Liberec, Bendlova, Czech Republic; [c]Department of Metals and Corrosion Engineering, University of Chemistry and Technology, Prague, Czech Republic; [d]Department of Botany, Faculty of Science, Charles University in Prague, Prague, Czech Republic

ABSTRACT

Carbon steel is currently being considered as a candidate canister material for use in a deep geological repository of radioactive waste. Assessment of canister material corrosion through microbial activity is an important part of the safety assessment for the final repository. The aim of study was to compare and characterise the corrosion behaviour of carbon steel under sterile and non-sterile anaerobic conditions in natural groundwater containing sulphate-reducing bacteria (SRB). A molecular-biological approach was used to determine the presence and abundance changes of relevant bacterial groups. Carbon steel corrosion rates were higher in the presence of SRB compared with sterile control. EIS described the evolution of three time-constants under non-sterile conditions, while scanning electron microscopy confirmed that the carbon steel surface was covered with a two-layer biofilm. Molecular-biological analysis of the water and biofilm indicated the dominance of SRB, with *Desulfomicrobium* and *Desulfovibrio* species prevalent.

ARTICLE HISTORY
Received 20 August 2019
Revised 28 November 2019
Accepted 29 November 2019

KEYWORDS
biofilm; corrosion; deep geological repository; electrochemical impedance spectroscopy; microbially influenced corrosion; radioactive waste repository; sulphate reducing bacteria

Introduction

Microorganisms can cause microbially influenced corrosion (MIC), also known as biocorrosion, on a wide range of materials [1]. There are numerous examples showing that MIC can result in higher corrosion rates than would normally be expected for a particular environment/material combination [2]. Such high corrosion rates can lead to the premature failure of individual components or compromise structural integrity [3]. In deep geological disposal a commonly accepted strategy for management and treatment of high level long-lived radioactive waste [4], a multi-barrier system is planned to ensure its long-term safe storage. This multi-barrier system consists of the host rock, clay material and the metal canister. Although one of the main roles of the buffer clay material is to reduce microbial activity, it has repeatedly been shown that microbial activity cannot be suppressed completely [5–10]. In such cases, the metal canister, whose main role is to prevent radionuclides being released into the surrounding environment, may be threatened by MIC [9,10]. Since the protective function of the clay buffer is not absolute, it is essential that the corrosion behaviour of the confining material is fully understood in order to ensure the overall safety of the disposal process [4,11].

In the Czech Republic, the general concept of deep geological repository is based on the Swedish KBS-3 concept with certain modifications, for example the repositories are constructed in crystalline host rock using steel-based disposal canisters and bentonite as a buffer material [12], with the metal canisters being embedded several hundred metres below ground level [13]. It has already been demonstrated that microorganisms are present and metabolically active in such deep underground ecosystems [14–17]. The so-called deep biosphere is devoid of oxygen, hence microorganisms use nitrate, manganese, iron, sulphate or carbon dioxide as terminal electron acceptors for respiration, or gain energy through fermentation processes [18]. Sulphate-reducing bacteria (SRB) are typical anaerobes that utilise sulphate as a terminal electron acceptor and organic compounds and hydrogen as electron donors and a source of energy. Under anoxic conditions, which will prevail for most of the repository's lifetime, SRB gain energy by reduction of sulphate or other sulphur compounds to form hydrogen sulphide (H_2S), an aggressive corrosive element that can seriously threaten the integrity of metal canisters by accelerating their corrosion rate [19]. The electron donor is either a hydrogen ion (evolved either as a metabolic product of other bacteria or by hydrolysis due to the corrosion process) or an organic compound [20]. In addition to SRB, other bacterial groups (e.g. thiosulfate-reducing bacteria, nitrate-reducing bacteria, acetogenic bacteria) are also known for their ability to participate in biocorrosion [21–26]. However, SRB are considered to play a key role in the anaerobic corrosion of iron [27–30] as they are widespread in many natural and engineered environments. It has been demonstrated that interface locations between the buffer and other mbkaterials (i.e. at locations constituting a discontinuity in the homogeneity of the buffer) are clearly preferred environments for microbial activity as water content is higher and dry density of the buffer material lower than in the bulk buffer [31]. Since such interfaces will exist between the metal canister and the buffer material, microbial activity is expected to be higher at such locations, possibly resulting in MIC.

After closure of a repository in which an anoxic environment has evolved, localised corrosion may be induced by the activity of anaerobic microorganisms (mainly SRB).

CONTACT Tomáš Černoušek tomas.cernousek@cvrez.cz Department of Nuclear Fuel Cycle, Research Center Řež, Řež 130, Husinec 250 68, Czech Republic
© 2019 Institute of Materials, Minerals and Mining Published by Taylor & Francis on behalf of the Institute

Such localised MIC attack mostly results in pitting, with more generalised corrosion occurring later [11,32]. SRB promote anaerobic corrosion of iron via two basic mechanisms, namely indirect and direct. The indirect mechanism (also called chemical microbially induced corrosion; CMIC; e.g. [20]) is a chemical attack by hydrogen sulphide, which is faster than that by water and promotes so-called hydrogen embrittlement of the metal. Under the direct mechanism (also called electrical microbially influenced corrosion; EMIC; e.g. [20]), SRB stimulates corrosion by scavenging 'cathodic hydrogen' or a 'hydrogen film' on water-exposed iron [20,33]. Both mechanisms may occur simultaneously to differing extents [33].

Microorganism activity usually occurs in biological films (biofilms), composed of different microorganisms, and organic and inorganic materials [32]. These biofilms have a unique ability to adapt and survive under extreme values of pH, temperature, redox potential, salinity, pressure and radiation. Microorganisms near metal surfaces attach themselves through the production of extracellular polymeric substances (EPS). Interactions between the metal surface and the biofilm may then alter the kinetics of anodic/cathodic reactions occurring during electrochemical processes. Biofilm formation may enhance metal deterioration [34] by affecting the physico-chemical properties of the metal surface or by altering the properties of the passivation layer [11]. On the other hand, biofilms can also have a passivation effect, protecting the metal surface against corrosion [35].

Over the last decade, several studies have reported MIC on stainless steel, carbon steel and P235GH steel materials under repository relevant conditions [4,34–37]. A recent study on MIC of carbon steel exposed to anaerobic soil using conventional electrochemical techniques demonstrated localised corrosion on the steel surface accompanied by breakdown of the biogenic ferrous sulphide (FeS) film [38]. Similarly, a study on carbon steel corrosion in a deep groundwater environment containing bacteria described pitting corrosion caused by microbial activity. During this three-month study, a corrosion rate of 1.4 $\mu m \cdot a^{-1}$ of carbon steel coupon was described at room temperature and 11.4 $\mu m \cdot a^{-1}$ at 6°C [39]. While a further study also noted biofilm formation on carbon steel exposed to SRB, the experiment only lasted 35 days, which limited the corrosion behaviour observed [34]. Overall, these studies were subject to a number of methodological shortcomings, such as lack of microbial analysis and/or sterile control conditions and inadequate exposure time.

In order to better understand the processes outlined above, we undertook a series of experiments lasting 240 days in both non-sterile (i.e. groundwater containing SRB) and sterile anaerobic conditions. The experiments were designed to (a) determine and understand the contribution of biocorrosion to overall corrosion, and (b) determine microbial community composition and describe the bacteria responsible for corrosion and biofilm formation using molecular biological approaches.

Experimental procedures

Material and groundwater samples

Circular test plates, measuring 15 mm in diameter and 3 mm thick, were constructed of commercial C15E low carbon steel (wt-%, 0.15 C, 0.58 Mn, 0.256 Si, 0.029 S, 0.06 P, and Fe balance; see Figure 1). For the corrosion experiment, the plate surface was mechanically polished with P500 silicon carbide grinding paper in an Argon-purged glove box, following which the plates were cleaned with de-aerated ethanol. Natural groundwater was collected at a depth of approximately 100 m from the VITA source at the Josef Underground Research Centre (Czech Republic; chemical composition provided in Table 1). The water is naturally anaerobic and contains a microbial consortium dominated by SRB. A sterile abiotic control was obtained through sterile filtration of the same groundwater through a membrane filter with a pore size of 0.22 µm [40].

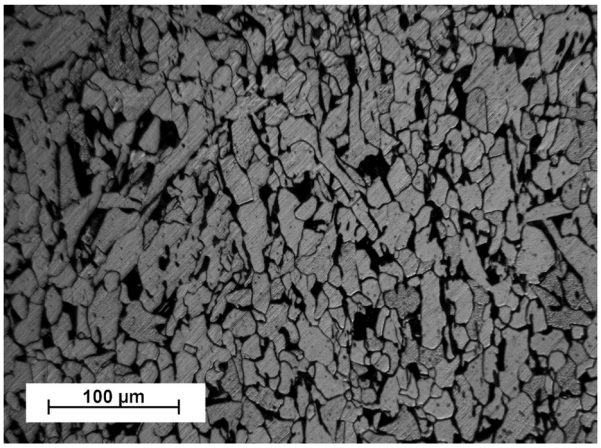

Figure 1. Microphotograph of the carbon steel sample.

Electrochemical measurement

The corrosion experiment was carried out in an argon-purged glove box (gaseous oxygen concentration <1 ppm volume) at approximately 25°C for 240 days. Open circuit potential (OCP or corrosion potential) measurement and electrochemical impedance spectroscopy (EIS) was undertaken weekly using a Gamry Reference 600 potentiostat/galvanostat/ZRA (GAMRY, USA), in order to characterise the corrosion process over the 240-day exposure period. Electrochemical measurements were performed with a three-electrode system, using a saturated calomel electrode as reference and two graphite rods as auxiliary electrodes Figure 2. The working electrode had an exposed metal surface area of 1 cm^2. The EIS tests were performed with a sinusoidal signal of 10 mV amplitude over a frequency range of 100 kHz–5 mHz at the corrosion potential. Later measurements, performed in order to gain information on polarisation resistance under non-sterile conditions, had an increased frequency range from 100 kHz to 10 µHz. Corrosion potential was highly stable and allowed EIS measurement at lower frequencies. Analysis of impedance spectra was performed using Gamry Echem Analyst 6.24 and ZSimpWin 3.50 software.

Surface and cross-section analysis

The steel specimen surfaces were examined after 240-days exposure using a LYRA3 scanning electron microscope (SEM; Tescan, Czech Republic). Changes in surface morphology were observed with secondary electron detectors (SE and In-beam SE mode) and back-scattered electrons (In-beam BSE mode) at 5 kV accelerating voltage. Energy-dispersive X-ray spectroscopy (EDS) was used to determine

Table 1. Chemical composition of the VITA natural groundwater.

Analyte	Concentration [mg L^{-1}]	Detection limit [mg L^{-1}]
Mg^{2+}	12.6	<0.1
Ca^{2+}	60	<0.1
Na^{+}	54.7	<1
K^{+}	1.79	<0.1
Fe^{2+}	1.01	<0.02
Mn^{2+}	0.11	<0.005
Cr^{3+}	<0.005	<0.005
TOC	97.0	<1
NH_4^+	<0.05	<0.05
Cl^-	16.6	<2
NO_2^-	<0.05	<0.05
NO_3^-	<2	<2
SO_4^{2-}	56.4	<10
PO_4^{3-}	1.0	<0.05
F^-	< 0.05	< 0.05
H_2S	0.08	< 0.01
Parameter	value	
Conductivity [mS cm^{-1}]	61.1	
pH	7.2	

local chemical composition using unprepared samples. Subsequently, the samples were modified by pouring into polyacrylic resin followed by cutting and polishing, after which they were carbon sputtered to a thickness of 10 nm to provide charging reduction. Cross-section analysis was then performed at 20 kV accelerating voltage.

Cross-section analysis of corrosion penetration was carried out using an Olympus PME3 metallographic microscope equipped with AxioVision software. Micro-Raman analysis was then performed using a Thermo Scientific DXR2xi spectrometer with a 532 nm laser line coupled with an optical microscope using a 10× magnification objective lens. Laser power was set at 0.5 mW in order to minimise possible phase transition of corrosion products.

Molecular biological analysis

DNA extraction and quantification

DNA was extracted from freshly collected underground water (VITA), test water and any biofilm forming on the surface of the carbon steel at the end of the experiment (240 days). Bacteria from the water samples was concentrated for subsequent analysis by filtering through a 0.22 µm GV Durapore® filter membrane under sterile conditions. Biofilm samples from the metal's surface were collected using sterile swabs. Genomic DNA from the membrane filters and biofilm were extracted using the MO BIO PowerWater DNA Isolation Kit (MO BIOLaboratories, Carlsbad, CA, USA) following the protocol provided by the manufacturer. Extracted DNA was quantified using a Qubit 2.0 fluorometer (Life Technologies, CA, USA).

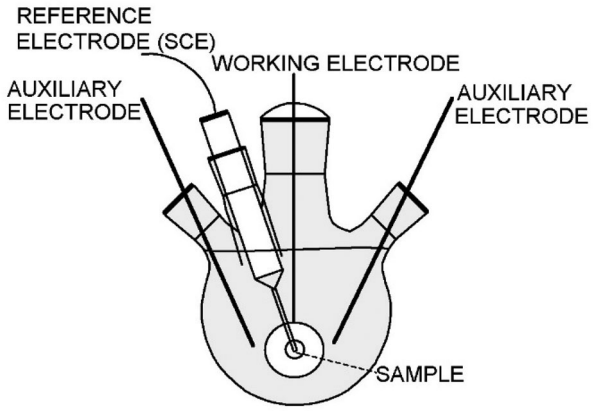

Figure 2. Experimental corrosion cell.

Quantitative polymerase chain reaction analysis

Quantitative polymerase chain reaction (qPCR) analysis was used to determine changes in the relative abundance of SRB by detecting gene levels for the adenosine-5′-phosphosulphate reductase (apsA) and dissimilatory sulphite reductase (dsr A) genes [41]. Both the apsA and dsr A genes are functional markers for SRB. Similarly, the 16S rDNA gene was used to monitor changes in total bacterial biomass using the 16s rRNA primer [42]. The 16S rRNA gene is a molecular marker for identifying the relative abundance of bacterial biomass. qPCR was performed on a Light Cycler® 480 (Roche, Switzerland), with reaction mixtures prepared in 10 µL of reaction volume. The mixture contained 2 µL of DNA template, 5 µL KAPA SYBER FAST qPCR kit (Kapa Biosystems. Inc., MA, USA), 0.4 µL of 20 µM forward and reverse primer mixtures (Generi Biotech, Czech Republic, IDT, US) and 2.6 µL ultra-pure water (Bioline, UK). Two parallel qPCR reactions were conducted for each DNA sample, along with a control with no DNA template. Reaction conditions comprised an initial 5 min incubation at 95°C, followed by 45 cycles of denaturation at 95°C for 10 s, annealing at 60°C for 15 s and extension at 72°C for 20 s, with a final extension at 72°C for 3 min. Finally, a melting curve was set for 5 s at 95°C, 1 min at 65°C, then ranging from 60 to 98°C with a temperature gradient of 40°C per 10 s. Purity of the amplified fragment was determined through observation of a single melting peak. Crossing point values were obtained using the 'second derivative maximum' method included in the LightCycler® 480 Software. This method has different amplification efficiencies for each primer, with individual amplification efficiency determined by measuring the slope of curves constructed from a serial dilution of template DNA from five environmental internal standards. During the evaluation process, each water sample was normalised to dilution and the total amount of DNA extracted. The relative abundance of the bacterial 16S rDNA gene and apsA and dsrA genes was calculated and expressed as a fold change between initial and end of sampling time using the delta Cp method. Using this method, each molecular biological marker is considered separately and the trends in relative abundance observed over time.

Next generation sequencing

The DNA extracted from the filter and biofilm samples (as described above) was used for 16S rRNA gene amplicon sequencing. Two consecutive PCR reactions were performed per sample in order to amplify the V4 region of the bacterial 16S rRNA gene, using normal and barcode fusion primers. *In silico* analysis of primers was conducted the amplicon size kept below 400 bp in order to cover as much microbial diversity as possible. Amplification of the 16 S rDNA gene itself was undertaken using the primers 530F [43] and 802R [44]. PCR conditions for the first PCR run were as follows: 95°C for 3 min; 10 cycles at 98°C for 20 s, 50°C for 15 s and 72°C for 45 s, and a final extension at 72°C for 1 min. The second PCR run was performed as follows: 95°C for 3 min; 35 cycles at 98°C

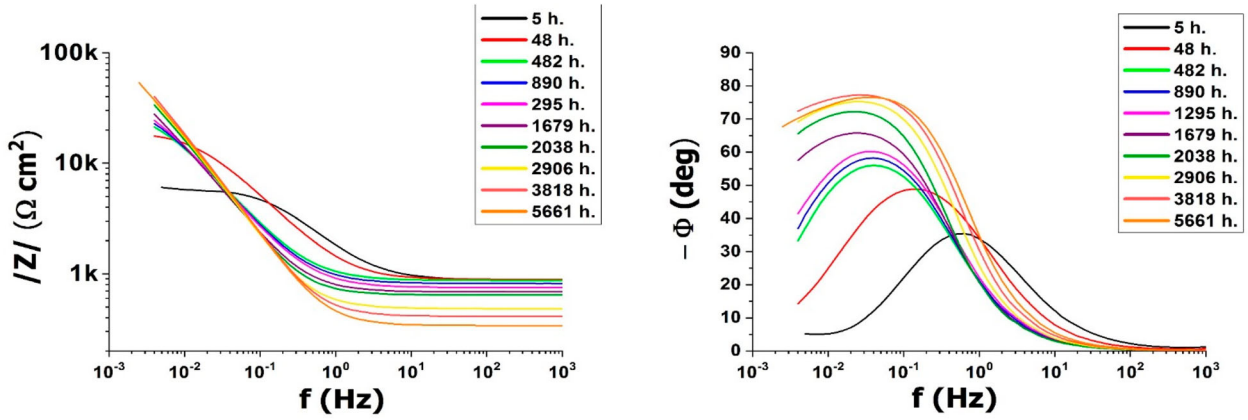

Figure 3. Bode plots of electrochemical impedance spectra time evolution for carbon steel under sterile conditions.

for 20 s, 50°C for 15 s and 72°C for 45 s, with a final extension at 72°C for 1 min. PCR products were purified using the Agencourt Ampure XP system (Beckman Coulter, Brea, CA, USA), the concentration of the purified PCR product being measured with a Qubit 2.0 fluorometer (Life Technologies, USA). Subsequently, the barcode-tagged amplicons from different samples were mixed in equimolar concentrations. Templating and enrichment for sequencing was performed using the One-Touch 2 and One-Touch ES systems (Life Technologies, USA), with sequencing of the amplicons performed on the Ion Torrent Personal Genome Machine (PGM) using the Ion PGM Hi-Q Sequencing Kit with the Ion 314 Chip v 2 (Thermo Fisher Scientific), following the manufacturer's instructions.

The raw Ion Torrent reads were processed using Mothur software v 1.39.5 [45], with high quality reads and reads with a length between 200 and 400 bp only used for further analysis. These settings produced 269,508 reads with an average length of 268 bp. Mothur pipeline settings were verified using a MOCK community sample. Chimeric sequences were identified using the VSEARCH algorithm [46] and subsequently removed. The sequences were then classified against the Silva database v 123, using 80% as a bootstrap value, and clustered into operational taxonomic units using an identity threshold of 97%. Cluster analysis was undertaken using the Vegan package in the R statistical software package [47]. Only those taxa with a relative abundance over 1% were visualised.

Results and discussion

Electrochemical impedance spectroscopy

Time evolution of impedance spectra, measured under both sterile and non-sterile conditions, is provided as Bode representations in Figures 3 and 4. High phase shift values at a frequency range of 100 kHz to 1 kHz appear to be artefacts caused by a parasitic capacitance originating from the electrochemical cell. Consequently, this part of the spectra was disregarded during further analysis. Spectra measured under sterile conditions are characterised by a single capacitive time constant over the whole measurement period, indicating uniform corrosion of the carbon steel. This corrosion stage is modelled in the circuit description code by the equivalent circuit R1(R2Q1), where R1 is the solution resistance, R2 is the polarisation resistance and Q1 is the dispersive double-layer capacitance characterised by the constant phase element. Table 2 shows selected results for EIS measurements

Table 2. Results of EIS measurements performed under sterile conditions.

Element → Time (h) ↓	*R*1 [Ohm cm^2]	*Q*1 [Ω^{-1} s^{-n} cm^{-2}]	*n*1	*R*2 [Ohm cm^2]
5	872	1.75E−04	0.7862	5198
48	876.4	2.76E−04	0.7739	19,430
482	867.2	5.76E−04	0.8081	32,170
890	814.7	5.99E−04	0.8195	36,710
1295	747.5	6.10E−04	0.8243	42,770
1679	681.5	7.05E−04	0.8473	82,160
2038	640.5	7.19E−04	0.8949	127,700
2906	484.3	7.13E−04	0.9100	157,300
3818	412.4	6.79E−04	0.9191	208,500
5661	301.6	7.01E−04	0.9082	209,600

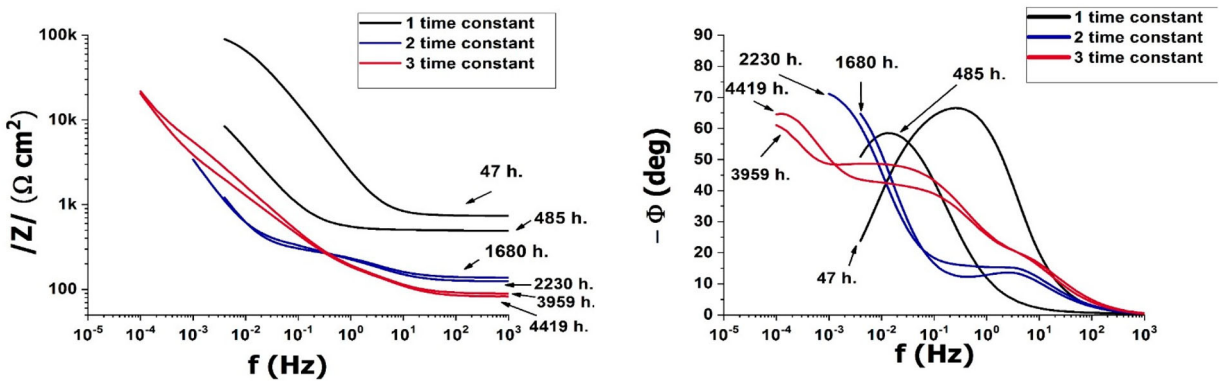

Figure 4. Bode plot of electrochemical impedance spectra time evolution for carbon steel under non-sterile conditions.

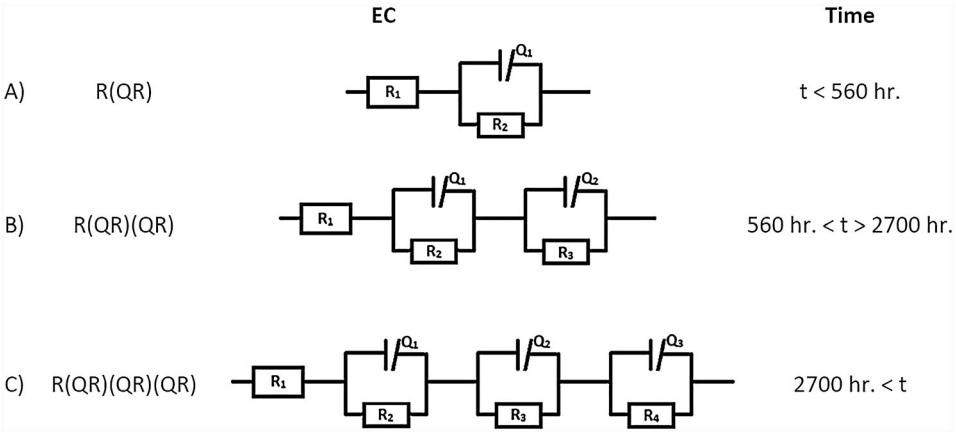

Figure 5. Equivalent circuits used for EIS data fitting and time evolution of corrosion stages.

Table 3. Results of EIS measurements performed under non-sterile conditions.

Element → Time (h) ↓	R_1 [Ohm·cm^2]	Q_1 [$\Omega^{-1}s^{-n}$ cm^{-2}]	n_1	R_2 [Ohm cm^2]	Q_2 [$\Omega^{-1}s^{-n}$ cm^{-2}]	n_2	R_3 [Ohm cm^2]	Q_2 [Ω^{-1} s^{-n} cm^{-2}]	n_3	R_4 [Ohm cm^2]
6	691	9.56E−05	0.7916	43,580						
47	724.8	9.71E−05	0.8411	105,600						
485	496.1	0.00195	0.7933	27,700						
866	308.4	0.0111	0.9356	17,300	0.0144	0.4866	297.4			
1295	206.8	0.01756	0.8993	25,710	0.00411	0.4387	102.2			
1537	142.6	0.02229	0.8983	30,390	0.00175	0.4864	175.8			
2230	100.1	0.02785	0.8932	63,370	0.0021	0.4639	298.8			
4239	80.32	0.05035	0.9358	85,130	0.00356	0.5608	22.65	0.00113	0.9792	3381
5080	82.21	0.02807	0.8554	125,800	0.00374	0.5904	20.06	0.0013	0.9781	6891

performed under sterile condition. The three equivalent circuits (Figure 5) were used sequentially for data fitting under non-sterile conditions, representing three corrosion stages. The first corrosion stage is characterised by one capacitive time constant, equivalent to the sterile environment, where R1 is the solution resistance, R2 is the polarisation resistance and Q1 is the dispersive double-layer capacitance.

Initial EIS measurements under both sterile and non-sterile conditions showed similar corrosion patterns characterised by the presence of a single time constant. In the non-sterile environment, the main differences observed were a more rapid increase in dispersive double-layer capacitance and a rapid decrease in solution resistance over time. A second corrosion stage was observed after 23 days, represented by the occurrence of two time constants due to biofilm formation. This corrosion stage was modelled in the circuit description code by the equivalent circuit R1(R2Q1)(R3Q2), where R3 represents resistance of the biofilm and Q2 is dispersive capacitance of the biofilm. Values n2 of dispersive capacitance Q2 indicating the influence of diffusion. The second biofilm time constant appeared in the high-frequency area. A third-time constant was observed after 112 days which is usually indicative for the change of the corrosion state on the surface. This was confirmed by the results of SEM measurements (see below) revealing the presence of the second biofilm layer. The formation of the second biofilm layer caused a shift in Faradaic charge transfer to very low frequencies of up to tens of μHz linked to an increased contribution of diffusion resistance. This corrosion stage was modelled in the circuit description code by the equivalent circuit R1(R2Q1)(R3Q2)(R4Q3), where R4 represents the resistance of the second biofilm and Q3 is the second biofilm's dispersive capacitance. The impedance of the second biofilm layer differed from that of the first by showing lowered value n3 and increased capacitance. Table 3 shows selected results for EIS measurements under non-sterile conditions. Approximation accuracy of the experimental data by each equivalent circuit (χ^2-chi-square goodness of fit test) achieved similar values in sterile and non-sterile environments, ranging in the order of 10^{-4} to 10^{-5}.

The polarisation resistance time dependence under sterile and non-sterile conditions was estimated by fitting nonlinear least squares (Figure 6). Increased polarisation resistance during the early stages of the experiment under non-sterile conditions can be attributed to sedimentation of solid particles (probably carbonates), which has an inhibitory effect on corrosion rate compared with the sterile environment without colloidal particles. When SRB were present, carbon steel polarisation resistance decreased by a factor of two after 240 days, when compared with sterilised VITA groundwater.

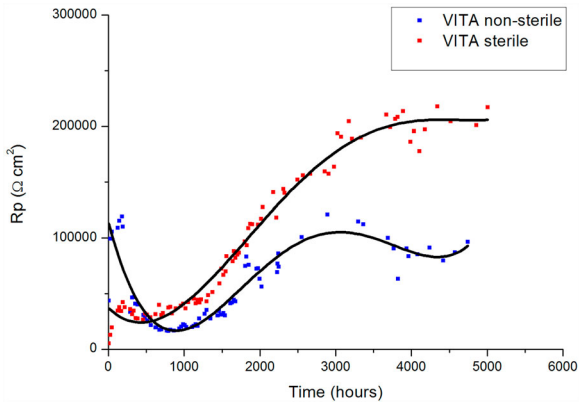

Figure 6. Time evolution of polarisation resistance.

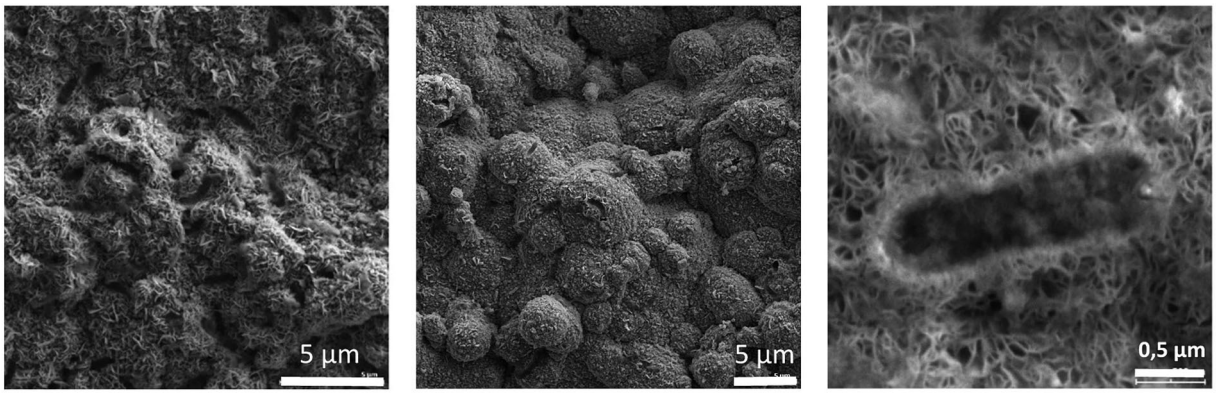

Figure 7. Scanning electron micrographs of the biofilm formed on carbon steel exposed under non-sterile conditions after 240 days incubation (SE detector).

Surface and cross-section analysis

SEM images indicated that the surface of carbon steel in the presence of bacteria was covered with a relatively thick layer of spherical and rod-shaped microorganisms with many cells visible (Figure 7). The biofilm consisted of microorganisms surrounded and held together by an excreted gelatinous matrix of EPS composed of high molecular weight compounds [48, 49]. The bacteria were about 2 µm long and had a typically cylindrical shape. The SE detector mode provided the best surface visualisation, showing the bacteria as dark rod-shaped objects (Figure 8). The main disadvantage of this mode was the difficulty in finding bacterial cells. Use of the BSE detector improved the imaging contrast between bacterial cells (comprising elements of lower atomic number) and the steel's surface due to the backscatter of electrons, which made areas where bacteria were located appear darker (Figure 8). Surface analysis showed a heterogeneous sample surface with some areas covered with biofilm and some with many flat crystals.

Local EDS analysis demonstrated that the corrosion products were mainly composed of iron, oxygen, sulphur and carbon. This finding was supported by elemental maps of those areas with bacteria present (Figure 9). The presence of sulphur and iron suggests iron sulphide minerals

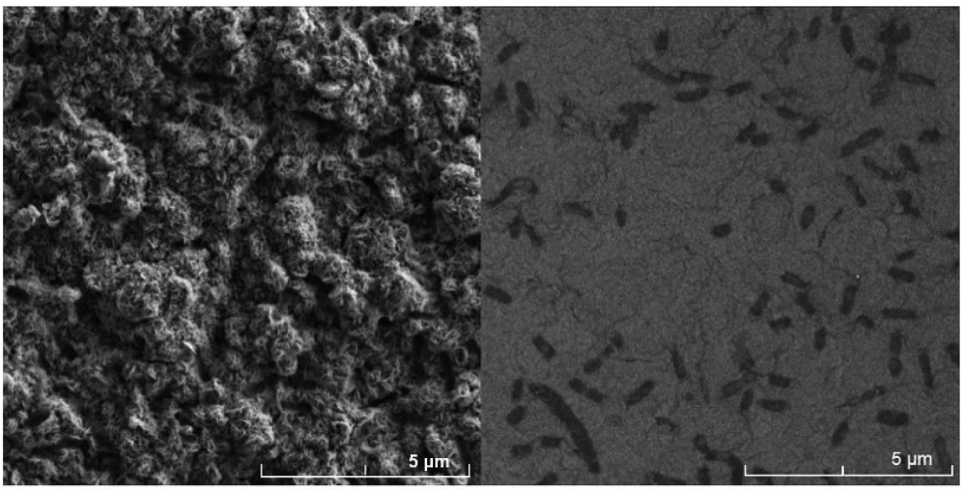

Figure 8. Scanning electron micrograph of the biofilm formed on carbon steel exposed under non-sterile conditions after 240 days incubation – comparison of different detector modes (left SE detector, right In-Beam BSE detector).

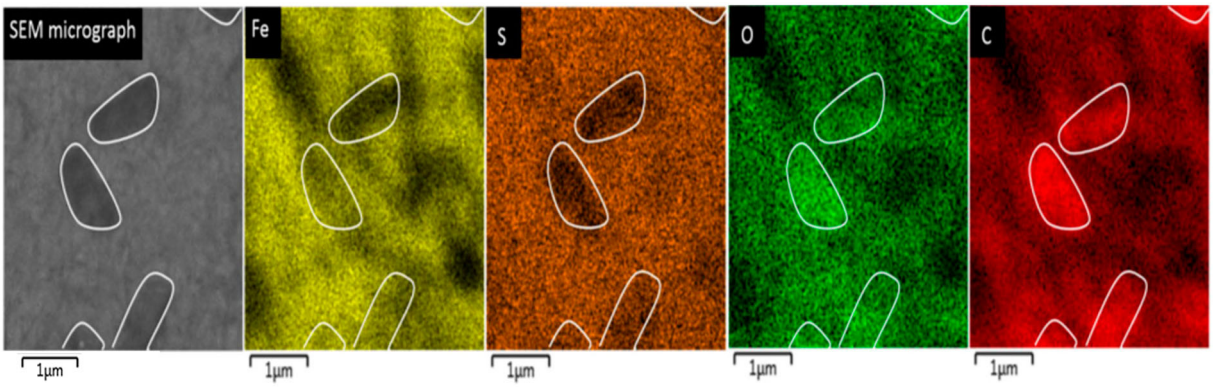

Figure 9. Energy-dispersive X-ray elemental maps of the corroded region with bacteria present (marked with a white line).

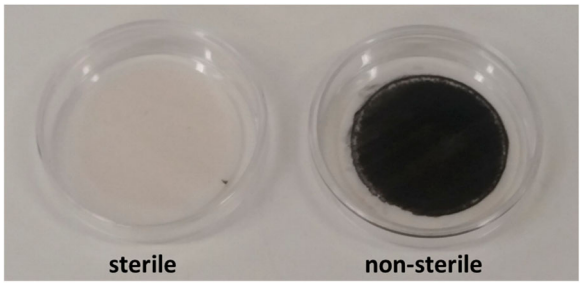

Figure 10. Comparison of filters after filtration of the water used for the experiment. Left: sterile negative control, right: non-sterile sample.

formation, thereby indicating bacterial activity. Additionally, black turbidity was observed in the experimental cell (see Figure 10) and on the surface of the testing coupon under non-sterile conditions. In contrast, no sulphur or signs of microbial activity were detected by SEM/EDS on the sample under sterile conditions. SEM analysis indicated that the covering layer was stratified into a thicker (approx. 24.5 µm) inner layer (labelled 2 in Figure 11) and a thinner (approx. 3.7 µm) outer layer (labelled 1 in Figure 11), representing dry film thickness. The composition of these layers differed, with the inner layer being dominated by iron and oxygen with a small amount of sulphur and the outer layer comprising iron with oxygen with sulphur dominating for the EDS spectra (the point labelled 3 in Figure 11 was dominated by silicon).

The cross-section images given in Figure 12 show that corrosion penetration is much lower and thickness more homogeneous in the sterile sample, and much thicker and less homogeneous in the non-sterile sample (evaluation summary in Table 4). The average penetration for the sterile sample was 8.36 and 27.80 µm for the non-sterile sample, while maximum penetration was 14.01 µm for the sterile sample and 61.31 µm for the non-sterile sample. Extreme penetrations observed at the non-sterile sample surface are probably caused by occluded solution formation under the biofilm, with subsequent localisation of the corrosion attack.

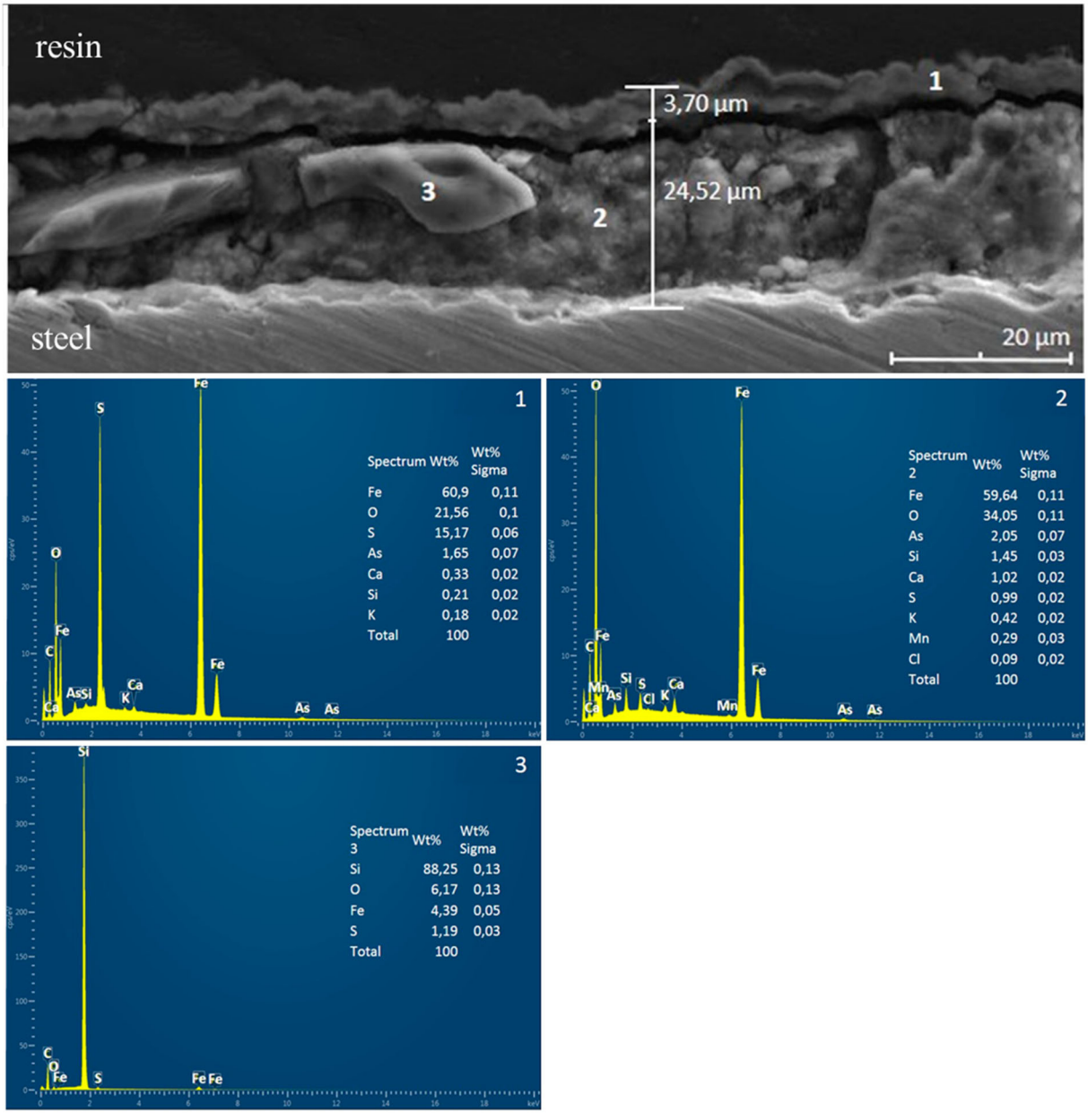

Figure 11. Scanning electron micrograph showing the formation of a corrosion layer. The image shows a sample cross section with bacteria present (above) and the respective X-ray spectra of positions 1, 2 and 3 (below).

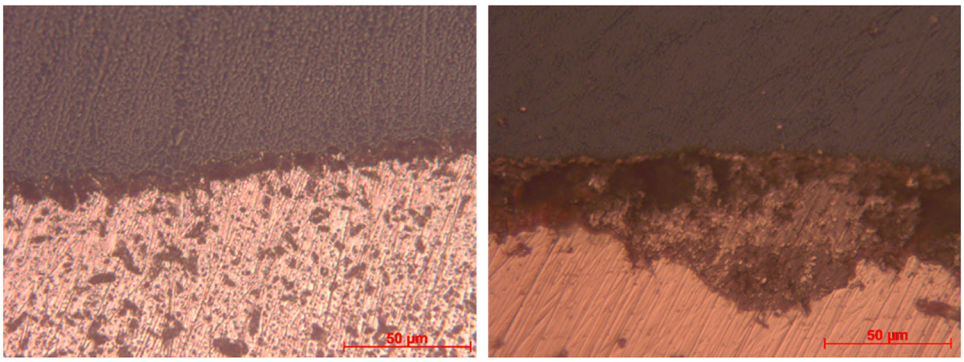

Figure 12. Cross sections of the sterile (left) and non-sterile (right) steel after exposure.

Table 4. Evaluation of corrosion penetration on cross-cut samples at the end of the experiment.

	Corrosion penetration (µm)			
Environment	Average	Standard deviation	Minimum	Maximum
Sterile	8.36	2.69	3.49	14.01
Non-sterile	27.80	10.74	10.46	61.31

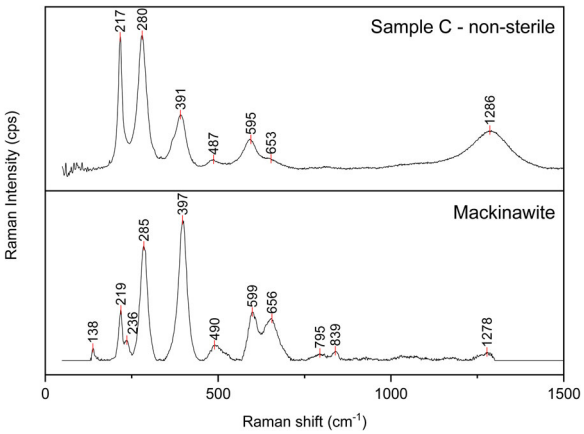

Figure 13. Raman spectra of carbon steel under non-sterile anaerobic conditions in VITA water after 293 days (top) and mackinawite standard (bottom).

Sterile and non-sterile samples were also analysed by micro-Raman spectroscopy, which detected the presence of mackinawite ($Fe_{1+x}S$) on the surface of the samples exposed to bacteria (characterised by peaks at 217, 280, 391, 487, 595, 653 and 1286 cm^{-1}; Figure 13). Mackinawite and greigite (Fe_3S_4) are a corrosion product typically reported from systems exposed to SRB and is therefore considered an indication of microbial activity on the surface of the material [50].

Microbial community analysis

Results of qPCR analysis indicated that the relative abundance of bacterial biomass (detected by the universal 16S rDNA marker) in the water sample increased slightly compared with the start of the experiment (Figure 14). In contrast, the amount of SRB in the water sample decreased approximately fivefold after 240 days (Figure 14). However, when interpreting these results, it should be taken into account that most bacteria contributing to MIC are expected to grow in the biofilm. No bacteria were detected by qPCR under sterile conditions.

Microbial composition of the test water and biofilm after 240 days was determined alongside the initial VITA groundwater source using NGS amplicon sequencing. The initial VITA water was dominated by mesophilic and thermophilic SRB such as *Desulfobacula*, *Desulfomicrobium*, *Desulfovibrio* and *Desulfurivibrio* (all Deltaproteobacteria). The genera *Paludibacter* (Bacteriodetes) and *Thiobacillus* (Betaproteobacteria), along with members of the Rhodocyclaceae and Comamonadaceae families (both Betaproteobacteria), were also common in VITA water. While the taxonomic composition of the microbial community present in both water and biofilm samples collected after 240 days changed, the communities were still dominated by SRB (Figure 15). While both *Desulfobacula* and *Desulfurivibrio* were detected at low numbers in the 240-day water and biofilm samples, *Desulfomicrobium* and *Desulfovibrio* spp. dominated in the biofilm sample. Members of these genera can utilise organic compounds or hydrogen as electron donors and sulphur compounds as electron acceptors [51,52] and, therefore they participate in MIC [20]. Both genera are also able to promote anaerobic corrosion indirectly (CMIC) through the corrosive chemical agent hydrogen sulphide. In addition, the genus *Desulfovibrio* includes many strains that have the

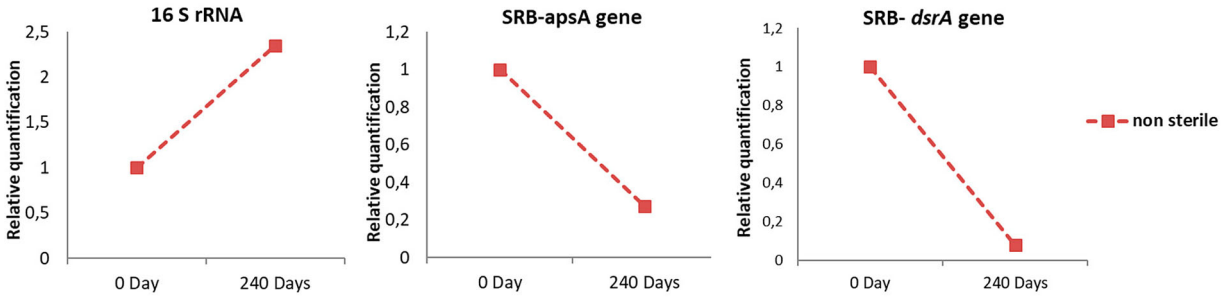

Figure 14. Results of qPCR analysis of the 16S RNA (total bacterial biomass) and *aps*A and *dsr*A genes (SRB), shown as relative change compared to the start of the experiment.

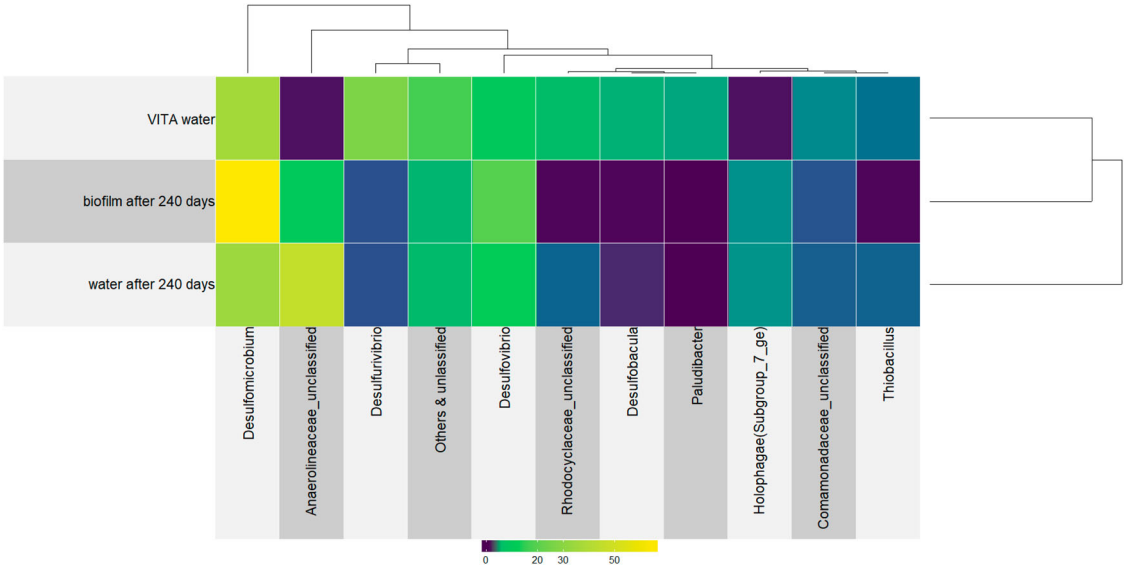

Figure 15. Heat map showing the results of next generation amplicon sequencing (only taxa with abundance over 1% visualised).

ability to corrode metals through direct withdrawal of electrons from the metal surfaces [20,33,53]. Under nutrient limiting conditions, as found in the groundwater examined in this study, the concentration of organic electron donors is relatively low and, as a result, microbes probably attack the steel as it represents a good source of electrons for reduction of sulphate to sulphide [39].

The obligate anaerobes Anaerolinaceae, found in low numbers in the initial VITA water, were detected in relatively high numbers in samples collected after 240 days. Similarly, members of the class Halophagae (subgroup_7_ge; phylum Acidobacteria) were also found in both 240-day water and biofilm samples in higher quantities than at the beginning of the experiment. At the same time, the numbers of other bacteria present in the initial VITA water sample declined significantly (see Figure 15). Natural biofilms are composed of a wide variety of microbes, including bacteria, archaea and fungi. When multiple corrosion-causing species are present they will act synergistically, causing severe corrosion [35,54]. A recent study conducted on water from the Yucca mountains (USA), for example, showed a higher rate of corrosion in the presence of a mixed bacterial population (iron and sulphur reducing bacteria) than in the presence of single species [55].

Conclusions

Under strictly anaerobic conditions, exposure of carbon steel to natural VITA underground water containing SRB resulted in the formation of a biofilm and corrosion product layers, determined and verified by EIS and SEM. Molecular biological analysis of both water and biofilm indicated dominance of *Desulfomicrobium* and *Desulfovibrio* spp. (both SRB). In brief, the following conclusions can be drawn:

- Steel corrosion rates were higher in the presence of SRB compared with samples without bacteria.
- The formation of a biofilm on the steel surface accelerated and localised the corrosion process.
- Presence of mackinawite, a corrosion product usually attributed to SRB activity, was confirmed by Raman spectroscopy.
- *Desulfomicrobium* and *Desulfovibrio* spp. dominated in the biofilm.
- Detection of sulphur compounds by SEM/EDS provided evidence of reduction of sulphate to sulphide by SRB metabolic activity.
- Compared with steel under sterile conditions, the carbon steel polarisation resistance was decreased by a factor of two after 240 days in the presence of SRB, indicating a higher corrosion rate.
- During long-term experiments of MIC, determination of polarisation resistance using EIS required the use of very low frequencies (up to 10 μHz), owing to the increasing contribution of diffusion resistance from the biofilm.

Disclosure statement

No potential conflict of interest was reported by the authors.

Funding

This work was supported by the European Union's Euratom research and training program (Horizon2020) under grant agreement 661880. (Microbiology in Nuclear Waste Disposal – MIND). This presented work was supported by the Ministry of Education Youth and Sports – project LQ1603 Research for SUSEN. This work has been realized within the SUSEN Project (established in the framework of the European Regional Development Fund (ERDF) in project CZ.1.05/2.1.00/03.0108 and of the European Strategy Forum on Research Infrastructures (ESFRI) in the project CZ.02.1.01/0.0/0.0/15 008/0000293, which is financially supported by the Ministry of Education Youth and Sports – project LM2015093 Infrastructure SUSEN. Part of this work has been carried out in the framework of Pro-NanoEnviCz project No. CZ.02.1.01/0.0/0.0/16_013/0001821. The work of Rojina Shrestha was supported by the Ministry of Education Youth and Sports through SGS project No. 21338/115 of the Technical University of Liberec.

ORCID

Tomáš Černoušek http://orcid.org/0000-0002-5584-4310
Rojina Shrestha http://orcid.org/0000-0002-7890-9383
Hana Kovářová http://orcid.org/0000-0002-1705-4035
Roman Špánek http://orcid.org/0000-0002-4854-3720
Alena Ševců http://orcid.org/0000-0001-8772-704X
Kristína Sihelská http://orcid.org/0000-0003-2760-9046
Jakub Kokinda http://orcid.org/0000-0001-8170-2247

Jan Stoulil http://orcid.org/0000-0002-3326-6011
Jana Steinová http://orcid.org/0000-0003-0229-4535

References

[1] Little BJ, Lee JS. Microbiologically influenced corrosion. Vol. 3. Hoboken (NJ): John Wiley & Sons Inc; 2007.
[2] Wade S, Mart P, Trueman A. Microbiologically influenced corrosion in maritime vessels. Corros Mater. 2011;36:68–79.
[3] Flemming HC. Economical and technical overview. In: Heitz E, Flemming HC, Sand W, editors. Microbially influenced corrosion of materials, scientific and engineering aspects. Berlin Heidelberg: Springer; 1996. p. 10–15.
[4] Libert M, Schütz MK, Esnault L, et al. Impact of microbial activity on the radioactive waste disposal: long term prediction of biocorrosion processes. Bioelectrochemistry. 2014;97:162–168.
[5] Stroes-Gascoyne S, Hamon CJ, Dixon DA, et al. Microbial analysis of samples from the tunnel sealing experiment at AECL's Underground Research Laboratory. Phys Chem Earth. 2007;32 (1):219–231.
[6] Stroes-Gascoyne S, Schippers A, Schwyn B, et al. Microbial community analysis of opalinus clay drill core samples from the Mont Terri underground Research Laboratory, Switzerland. Geomicrobiol J. 2007b;24(1):1–17.
[7] Masurat P, Eriksson S, Pedersen K. Microbial sulphide production in compacted Wyoming bentonite MX-80 under in situ conditions relevant to a repository for high-level radioactive waste. Appl Clay Sci. 2010;47(1–2):58–64.
[8] Smart NR, Rance AP, Reddy B, et al. In situ evaluation of model copper-cast iron canisters for spent nuclear fuel: a case of microbiologically influenced corrosion (MIC). Corros Eng Sci Technol. 2014;49(6):548–553.
[9] Smart NR, Reddy B, Rance AP, et al. The anaerobic corrosion of carbon steel in compacted bentonite exposed to natural Opalinus clay porewater containing native microbial populations. Corros Eng Sci Technol. 2017;52(sup1):101–112.
[10] Leupin OX, Bernier-Latmani R, Bagnoud A, et al. Fifteen years of microbiological investigation in Opalinus Clay at the Mont Terri rock laboratory (Switzerland). In: P Bossart, AG Milnes, editors. Mont Terri Rock Laboratory, 20 Years: Two decades of research and experimentation on claystones for geological disposal of radioactive waste. Cham: Springer International Publishing; 2018. p. 345–356.
[11] Schütz MK, Schlegel ML, Libert M, et al. Impact of iron-reducing bacteria on the corrosion rate of carbon steel under simulated geological disposal conditions. Environ Sci Technol. 2015;49 (12):7483–7490.
[12] Pospíšková I, Dobrev D, Kouřil M, et al. Czech national programme and disposal canister concept. Corros Eng Sci Technol. 2017;52(sup1):6–10.
[13] Pedersen K. Analysis of copper corrosion in compacted bentonite clay as a function of clay density and growth conditions for sulfate-reducing bacteria. J Appl Microbiol. 2010;108(3):1094–1104.
[14] Crozier R, Agapow P-M, Pedersen K. Towards complete biodiversity assessment: an evaluation of the subterranean bacterial communities in the Oklo region of the sole surviving natural nuclear reactor. FEMS Microbiol Ecol. 1999;28(4):325–334.
[15] Eydal H, Pedersen K. Use of an ATP assay to determine viable microbial biomass in Fennoscandian Shield groundwater from depths of 3–1000 m. J Microbiol Methods. 2007;70(2):363–373.
[16] Hallbeck L, Edlund J, Eriksson L. (2011). Microbial analyses of groundwater and surfaces during the retrieval of experiment 3, A04, in MINICAN, Swedish Nuclear Fuel and Waste Management Co.
[17] Pedersen K. Metabolic activity of subterranean microbial communities in deep granitic groundwater supplemented with methane and H_2. ISME J. 2012;7:839.
[18] Anderson C, Johnsson A, Moll H, et al. Radionuclide geomicrobiology of the deep biosphere. Geomicrobiol J. 2011;28(5–6):540–561.
[19] Pedersen K, Motamedi M, Karnland O, et al. Mixing and sulphate-reducing activity of bacteria in swelling, compacted bentonite clay under high-level radioactive waste repository conditions. J Appl Microbiol. 2000;89(6):1038–1047.
[20] Enning D, Garrelfs J. Corrosion of iron by sulfate-reducing bacteria: New views of an old problem. Appl Environ Microbiol. 2014;80(4):1226.
[21] Dowling NJE, Brooks SA, Phelps TJ, et al. Effects of selection and fate of substrates supplied to anaerobic bacteria involved in the corrosion of pipe-line steel. J Ind Microbiol. 1992;10(3):207–215.
[22] Magot M, Ravot G, Campaignolle X, et al. *Dethiosulfovibrio peptidovorans* gen. nov., sp. nov., a new anaerobic, slightly halophilic, thiosulfate-reducing bacterium from corroding offshore oil wells. Int J Syst Evol Microbiol. 1997;47(3):818–824.
[23] De Windt W, Boon N, Siciliano SD, et al. Cell density related H_c consumption in relation to anoxic Fe(0) corrosion and precipitation of corrosion products by Shewanella *oneidensis* MR-1. Environ Microbiol. 2003;5(11):1192–1202.
[24] Hubert C, Nemati M, Jenneman G, et al. Corrosion risk associated with microbial souring control using nitrate or nitrite. Appl Microbiol Biotechnol. 2005;68(2):272–282.
[25] Vik EA, Janbu AO, Garshol FK, et al. (2007). Nitrate based souring mitigation of produced water – side effects and challenges from the draugen produced water re-injection pilot. International Symposium on Oilfield Chemistry. Houston, Texas, Society of Petroleum Engineers.
[26] Xu D, Li Y, Song F, et al. Laboratory investigation of microbiologically influenced corrosion of C1018 carbon steel by nitrate reducing bacterium *Bacillus licheniformis*. Corros Sci. 2013;77:385–390.
[27] Booth GH. Sulphur bacteria in relation to corrosion. J Appl Bacteriol. 1964;27(1):174–181.
[28] Hamilton WA. Sulphate-reducing bacteria and anaerobic corrosion. Annu Rev Microbiol. 1985;39(1):195–217.
[29] Lee W, Lewandowski Z, Nielsen PH, et al. Role of sulfate-reducing bacteria in corrosion of mild steel: A review. Biofouling. 1995;8 (3):165–194.
[30] Beech IB, Sunner JA. Sulphate-reducing bacteria and their role in corrosion of ferrous materials. In: Barton LL, Hamilton WA, editors. Sulphate-reducing bacteria: environmental and engineered systems. Cambridge: Cambridge University Press; 2007. p. 459–483.
[31] Stroes-Gascoyne S. Microbial occurrence in bentonite-based buffer, backfill and sealing materials from large-scale experiments at AECL's Underground Research Laboratory. Appl Clay Sci. 2010;47(1):36–42.
[32] Féron D, Crusset D. Microbial induced corrosion in French concept of nuclear waste underground disposal. Corros Eng Sci Technol. 2014;49(6):540–547.
[33] Dinh HT, Kuever J, Mußmann M, et al. Iron corrosion by novel anaerobic microorganisms. Nature. 2004;427(6977):829–832.
[34] Paula MSd, Gonçalves MMM, Rola MAdC, et al. Carbon steel corrosion induced by sulphate-reducing bacteria in artificial seawater: electrochemical and morphological characterizations. Matéria (Rio de Janeiro). 2016;21(4):987–995.
[35] Kip N, Van Veen JA. The dual role of microbes in corrosion. ISME J. 2015;9(3):542.
[36] El Hajj H, Abdelouas A, Grambow B, et al. Microbial corrosion of P235GH steel under geological conditions. Phys Chem Earth Parts A/B/C. 2010;35(6–8):248–253.
[37] Valencia-Cantero E, Peña-Cabriales JJ. Effects of iron-reducing bacteria on carbon steel corrosion induced by thermophilic sulfate-reducing consortia. J Microbiol Biotechnol. 2014;24(2):280–286.
[38] Li S, Kim Y, Jeon K, et al. Microbiologically influenced corrosion of carbon steel exposed to anaerobic soil. Corrosion. 2001;57(9):815–828.
[39] Rajala P, Carpén L, Vepsäläinen M, et al. Microbially induced corrosion of carbon steel in deep groundwater environment. Front Microbiol. 2015;6:647.
[40] Madigan MT, Martinko JM, Bender KS, et al. Brock biology of microorganisms. 14th ed. Boston: Pearson; 2015.
[41] Ben-Dov E, Brenner A, Kushmaro A. Quantification of sulfate-reducing bacteria in industrial wastewater, by real-time polymerase chain reaction (PCR) using dsrA and apsA genes. Microb Ecol. 2007;54(3):439–451.
[42] Clifford RJ, Milillo M, Prestwood J, et al. Detection of bacterial 16S rRNA and identification of four clinically important bacteria by real-time PCR. PLoS One. 2012;7(11):e48558.
[43] Dowd SE, Callaway TR, Wolcott RD, et al. Evaluation of the bacterial diversity in the feces of cattle using 16S rDNA bacterial tag-encoded FLX amplicon pyrosequencing (bTEFAP). BMC Microbiol. 2008;8(1):125.

[44] Claesson MJ, Wang Q, O'Sullivan O, et al. Comparison of two next-generation sequencing technologies for resolving highly complex microbiota composition using tandem variable 16S rRNA gene regions. Nucleic Acids Res. 2010;38(22):e200–e200.
[45] Schloss PD, Westcott SL, Ryabin T, et al. Introducing Mothur: open-source, platform-independent, community-supported software for describing and comparing microbial communities. Appl Environ Microbiol. 2009;75(23):7537–7541.
[46] Rognes T, Flouri T, Nichols B, et al. VSEARCH: a versatile open source tool for metagenomics. PeerJ. 2016;4:e2584–e2584.
[47] Oksanen J, Blanchet FG, Kindt R, et al. Vegan: community ecology package. R Package Vegan, Vers. 2015;2:2–1.
[48] Bhaskar PV, Bhosle NB. Bacterial extracellular polymeric substance (EPS): A carrier of heavy metals in the marine food-chain. Environ Int. 2006;32(2):191–198.
[49] Reitner J. Microbial Mats. In: Reitner J, Thiel V, editors. Encyclopedia of Geobiology. London: Springer; 2011. p. 606–608.
[50] Remazeilles C, Saheb M, Neff D, et al. Microbiologically influenced corrosion of archaeological artefacts: characterisation of iron(II) sulfides by Raman spectroscopy. J Raman Spectrosc. 2011;41(11):1425–1433.
[51] Steger JL, Vincent C, Ballard JD, et al. *Desulfovibrio* sp. genes involved in the respiration of sulfate during metabolism of hydrogen and lactate. Appl Environ Microbiol. 2002;68(4):1932–1937.
[52] Dias M, Salvado JC, Monperrus M, et al. Characterization of *Desulfomicrobium salsuginis* sp. nov. and *Desulfomicrobium aestuarii* sp. nov., two new sulfate-reducing bacteria isolated from the Adour estuary (French Atlantic coast) with specific mercury methylation potentials. Syst Appl Microbiol. 2008;31(1):30–37.
[53] Venzlaff H, Enning D, Srinivasan J, et al. Accelerated cathodic reaction in microbial corrosion of iron due to direct electron uptake by sulfate-reducing bacteria. Corros Sci. 2013;66:88–96.
[54] Rajala P, Bomberg M, Vepsäläinen M, et al. Microbial fouling and corrosion of carbon steel in deep anoxic alkaline groundwater. Biofouling. 2017;33(2):195–209.
[55] Pitonzo BJ, Castro P, Amy PS, et al. Microbiologically influenced corrosion capability of bacteria Isolated from Yucca Mountain. Corrosion. 2004;60(1):64–74.